The Habc Domain and the SNARE Core Complex Are Connected by a Highly Flexible Linker

Martin Margittai,[‡] Dirk Fasshauer,[§] Reinhard Jahn,[§] and Ralf Langen*[,‡]

Department of Neurobiology, Max Planck Institute for Biophysical Chemistry, D-37077 Göttingen, Germany, and Department of Biochemistry and Molecular Biology, Zilkha Neurogenetic Institute, University of Southern California, Los Angeles, California 90089-2821

Received January 2, 2003

ABSTRACT: Syntaxin 1a is a member of the SNARE superfamily of small, mostly membrane-bound proteins that mediate membrane fusion in all eukaryotic cells. Upon membrane fusion, syntaxin 1 forms a stable complex with its partner SNAREs. Syntaxin contains a C-terminal transmembrane domain, an adjacent SNARE motif that interacts with its partner SNAREs, and an N-terminal Habc domain. The Habc domain reversibly folds back upon the SNARE motif, resulting in a "closed" conformation that is stabilized by binding to the protein munc18. The SNARE motif and the Habc domain are separated by a linker region of about 40 amino acids. When syntaxin is complexed with munc18, the linker is structured and consists of a mix of turns and small α-helices. When syntaxin is complexed with its partner SNAREs, the Habc domain is dissociated, but the structure of the linker region is not known. Here we used site-directed spin labeling and EPR spectroscopy to determine the structure of the linker region of syntaxin in the SNARE complex. We found that the entire linker region of syntaxin is unstructured except for three residues at the N-terminal and six residues at the C-terminal boundary whereas the structures of the flanking regions in the Habc domain and the SNARE motif correspond to the high-resolution structures of the isolated fragments. We conclude that the linker region exhibits a high degree of conformational flexibility.

SNARE[1] proteins constitute a superfamily of small membrane proteins that are thought to be key mediators in all fusion reactions in the secretory pathway of eukaryotic cells (*1*−*3*). Complex formation of SNARE proteins between opposing membranes is thought to tie the membranes closely together and thus to initiate membrane fusion (*4*). SNAREs are distinguished by heptad repeats of 60−70 amino acids, referred to as SNARE motifs (*5*, *6*). During complex formation the unstructured SNARE motifs assemble into elongated helix bundles of extraordinary stability (*7*−*10*). The crystal structures of two only distantly related SNARE complexes revealed a high degree of conservation (*11*, *12*). Accordingly, all SNARE core complexes consist of four different SNARE motifs, with each representing a distinct SNARE subfamily. According to the side chains in a conserved central layer of amino acids in the center of the bundle (three glutamines and one arginine), the subfamilies are designed Qa-, Qb-, Qc-, and R-SNAREs, respectively (*13*, *14*). After fusion, the SNARE complexes are disassembled by the ATPase NSF in conjunction with α-SNAP as cofactor (*15*).

The SNARE proteins acting in neuronal exocytosis are best characterized, and they therefore serve as paradigms for all SNARE proteins. They include the synaptic vesicle protein synaptobrevin 2 (VAMP) and the plasma membrane proteins syntaxin 1 and SNAP-25. Both synaptobrevin and syntaxin contain a single SNARE motif (R- and Qa-SNARE, respectively) and a neighboring transmembrane domain. In contrast, SNAP-25 contains two SNARE motifs (Qb- and Qc-SNARE motifs) connected by a loop region that is palmitoylated at multiple sites and anchors the protein to the membrane.

While assembly of SNARE motifs into core complexes appears to be central for the role of SNAREs in membrane fusion, many SNAREs including all Qa-SNARES contain N-terminal extensions that are independently folded. Structural studies of the isolated N-terminal domain of syntaxin 1 revealed an antiparallel three-helix bundle that is referred to as Habc domain [Figure 1 (*16*, *17*)]. Similar folds have been identified for the N-terminal domains of other syntaxins [but apparently also for some Qb-SNAREs such as vti1b (*18*)], suggesting that this structure is conserved despite high sequence divergence (*19*−*21*).

The Habc domain of syntaxin attracted considerable interest due to its potential function in regulating syntaxin's SNARE activity. In the isolated protein, this region reversibly binds to the SNARE motif of syntaxin. As a result, syntaxin switches between a "closed" conformation (Habc domain bound to the SNARE motif) and an "open" conformation (Habc domain free). Binding of syntaxin to munc18, a protein essential for exocytosis (*22*), arrests syntaxin in the closed conformation. Since in the closed conformation the SNARE

* To whom correspondence should be addressed. Phone: 323-442-1323. Fax: 323-442-2145. E-mail: langen@usc.edu.

‡ University of Southern California.

§ Max Planck Institute for Biophysical Chemistry.

[1] Abbreviations: SNARE, soluble NSF acceptor protein receptor; SNAP-25, synaptosome-associated protein of 25 kDa; NSF, *N*-ethylmaleimide-sensitive factor; EPR, electron paramagnetic resonance; NTA, nitrilotriacetic acid; PAGE, polyacrylamide gel electrophoresis.

10.1021/bi027437z CCC: $25.00
Published on Web 03/20/2003

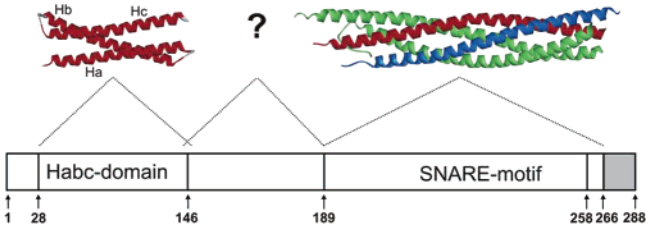

FIGURE 1: Mapping of syntaxin's high-resolution structures onto its primary sequence. The crystal structure of syntaxin's N-terminal domain is depicted on the left. The crystal structure of the protease-resistant ternary complex is shown on the right. Syntaxin is depicted in red, synaptobrevin in blue, and SNAP-25 in green. The domain structure of syntaxin is shown below. The arrows indicate domains of syntaxin. The first 27 amino acids of syntaxin are unstructured as observed by NMR spectroscopy. No structural information exists for the linker region of syntaxin that is bound to synaptobrevin and SNAP-25.

motif is unable to interact with other SNAREs, munc18 binding effectively prevents the formation of SNARE complexes (*23*, *24*). Although the ability to switch between open and closed conformations appears to vary considerably between different members of the syntaxin family (for review see ref *2*), an increasing body of evidence suggests that at least in syntaxin 1 this switch is important for exocytosis (*25*, *26*).

Insights into the associated conformational changes were obtained from the X-ray structure of the closed conformation of syntaxin complexed with munc18 (*27*). Although the structure of the Habc domain in this complex is very similar to that of the isolated domain, the structure of the SNARE motif [here also referred to as the H3 domain (*28*)], while mostly helical, differs from that in the SNARE complex. The structure of the munc18/syntaxin 1 complex also showed that the linker region connecting the Habc domain and the SNARE motif (amino acids 146−188) is structured in this complex. At the N-terminal boundary it extends the Hc helix to amino acid 155, i.e., almost three turns beyond the helix length observed in the isolated Habc domain. An additional small helix was observed between positions 162 and 170, which contacts not only munc18 but also the Habc and H3 domains.

Since aside from its C-terminal extension the structure of the isolated Habc domain is very similar to that in complex with munc18, it is probably the linker region that undergoes major conformational changes during the switch between closed and open conformation. When syntaxin is bound in the SNARE complex, the linker region is easily broken down by proteases (*29*, *30*). In addition, unfolding experiments of the homologous yeast SNARE complex revealed that the Habc domain and the SNARE complex behave as structurally separate entities (*31*). Finally, electron microscopy of isolated SNARE complexes (*32*) suggested that the relative positions of the Habc domain and the core complex are quite variable. Together, these findings suggest that in the SNARE complex the linker region is flexible, but no detailed structural information is available.

Here we have performed electron paramagnetic resonance (EPR) spectroscopy on syntaxin variants that were spin labeled at consecutive sites in the linker region and adjacent sites. Our results show that the linker region connecting the Habc domain and the SNARE motif is completely unfolded when syntaxin 1 is assembled with its SNARE partners, with gradual transitions at the interfaces to the adjacent Habc domain and the SNARE motif, respectively. We conclude that the linker region undergoes major conformational transitions during the switch between open and closed conformation and thus may constitute a target for conformational regulation.

EXPERIMENTAL PROCEDURES

Materials. Spin label [(1-oxy-2,2,5,5-tetramethylpyrrolinyl-3-methyl)methanethiosulfonate] was a kind gift of Kalman Hideg (University of Pecs, Hungary).

Plasmid Construction. The construction of plasmids harboring the sequences for synaptobrevin (1−96*)* and SNAP-25 (1−206, cysteines replaced by serines) was described elsewhere (*29*, *33*).

A cytosolic construct of syntaxin encompassing amino acids 1−262 in which the naturally occurring cysteine has been replaced by serine and which was cloned into pET28a via the *Nde*I/*Xho*I cleavage sites served as template for all new single cysteine constructs. Site-directed mutagenesis was performed according to the overlapping primer method using Pfu-DNA polymerase (*34*). Correctness of all sequences was checked for by DNA sequencing. The following constructs were obtained: Q138C, S139C, D140C, Y141C, R142C, E143C, R144C, S145C, K146C, G147C, R148C, I149C, R151C, L153C, E154C, T156C, R158C, T159C, T161C, S162C, E163C, E164C, L165C, E166C, D167C, M168C, L169C, E170C, S171C, G172C, N173C, P174C, A175C, I176C, F177C, A178C, S179C, G180C, I181C, I182C, M183C, D184C, S185C, S186C, I187C, S188C, K189C, Q190C, A191C, L192C, S193C, E194C, I195C, and T197C.

Protein Expression and Purification. Protein expression was induced in the BL21(DE3) strain of *Escherichia coli* by adding 0.8 mM IPTG to a bacterial culture grown in LB medium to OD_{600} ~0.8. Purification was essentially the same as described earlier (*35*). Briefly, the bacteria were pelleted and resuspended in extraction buffer (500 mM NaCl, 50 mM Tris, pH 7.4, 8 mM imidazole). The addition of 6 M urea helped in extracting the protein. Cells were sonified and subsequently incubated with Ni-NTA. After 1 h at 8 °C the Ni beads were washed with extraction buffer, and the recombinant protein was eluted with 400 mM imidazole (plus half of the extraction buffer). The N-terminal His tag was cleaved off by thrombin during overnight dialysis in 20 mM Tris, pH 7.4, 50 mM NaCl, and 1 mM DTT. After purification on Mono-Q (syntaxin and SNAP-25) and Mono-S (synaptobrevin) columns (Pharmacia/Amersham), all proteins were more than 95% pure as judged by SDS−PAGE analysis. Syntaxin was stored in a reducing environment by addition of 5 mM DTT prior to freezing.

Spin Labeling and SNARE Complex Formation. DTT was removed from the syntaxin mutants by gel filtration on PD-10 columns (Pharmacia/Amersham). Immediately after elution from the column (elution buffer: 20 mM HEPES, pH 7.4, 150 mM NaCl) syntaxin was reacted with a 10−20-fold molar excess of a cysteine-specific spin label [(1-oxy-2,2,5,5-tetramethylpyrrolinyl-3-methyl)methanethiosulfonate]. The reaction was allowed to continue for at least 1 h at room temperature. The mutants were concentrated in Microcons (MWCO: 10000), and excess spin label was removed by gel filtration (PD-10). In a final step, the proteins

were concentrated in Microcons. For SNARE complex formation a 2−4-fold molar excess of DTT-free synaptobrevin and SNAP-25 was added. Complex formation was allowed to proceed overnight on ice.

EPR Measurements. Prior to EPR analysis 30% sucrose was added to the complexes in order to reduce rotational tumbling. The concentration of spin-labeled syntaxin was in the range of 50−100 μM. All EPR spectra were obtained from an EMX spectrometer from Bruker. The field modulation that was applied for all samples was 1.5 G. The scan width was always 100 G. All spectra were normalized to the same number of spins. Spectral analysis was performed with software generously provided by Dr. Christian Altenbach.

Our approach is largely based on the ability to interpret the shape of the first derivative spectra in terms of the mobility of the spin label (for review see refs *36*−*39*). Depending on whether the label is positioned in a loop, on a structured surface, whether it has tertiary contacts, or whether it is completely buried, it yields characteristic spectra that in conjunction with data from neighboring sites allow determining structure at the level of the backbone fold. EPR spectroscopy has recently been demonstrated to be a powerful tool in examining SNARE structure (see, for example, refs *35*, *40*, and *41*).

RESULTS

The Habc Domain. In the first series of experiments, we investigated the structure of the Habc domain of syntaxin 1 in fully assembled SNARE complexes. Both in isolation and in complex with munc18 the domain resembles an up-and-down three-helix bundle (*16*, *17*, *27*), suggesting that it represents a stable fold, which does not change during the conformational transitions. Here, we examined whether this is also true for the assembled SNARE complex. In particular, we were interested in the C-terminal end of the Habc domain where in the munc18 complex the helix is extended in comparison with the structure of the isolated domain.

Eight consecutive residues covering the C-terminal end of the Hc helix (residues 138−145) and two additional positions in the middle of the Habc domain (residues 59 and 121) were spin labeled and measured either in free syntaxin or in the assembled SNARE complex (Figure 2). Both sets of data resulted in nearly superimposable spectra (Figure 2 depicts the spectra of the corresponding SNARE complexes), suggesting that the structures are very similar. Position 138, which points into the helix bundle, results in a broad EPR spectrum characteristic of an immobilized spin label. Residues 141 and 145, which also point toward the interior, show mobile components in addition to immobile peaks, indicating higher motional freedom toward the end of the helix. All other C-terminal positions resemble helix surface sites (residues 139, 140, 142, 143, and 144), in good agreement with the crystal and NMR structures, with residues 139, 143, and 144 that point away from the bundle in the high-resolution structures yielding the lowest central line widths (see also Figure 6).

Similarly, the spectra obtained for the middle positions (residues 59 and 121) are in good agreement with the high-resolution structures and confirm that the fold of the Habc domain remains unchanged upon formation of SNARE complexes. In all high-resolution structures these positions

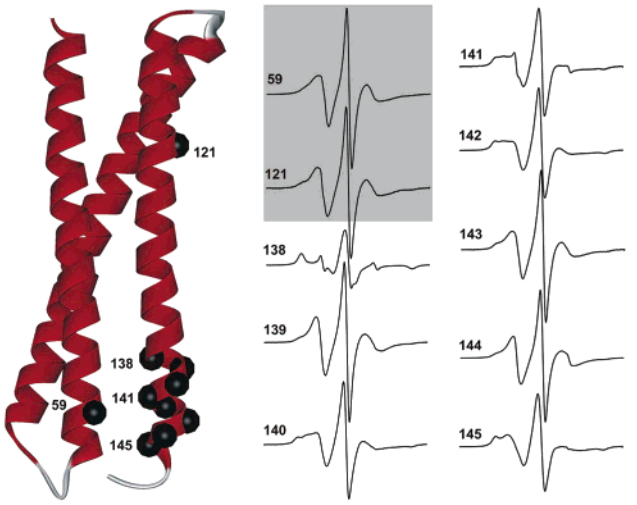

FIGURE 2: EPR spectra of syntaxin in complex with synaptobrevin and SNAP-25 spin labeled at the C-terminal end and two additional positions of the Habc domain. Positions that are labeled are mapped onto the crystal structure (left). Depicted are the α-carbons of the corresponding amino acids (black spheres).

represent exposed helix surface sites. Accordingly, the EPR spectra for both positions are characterized by narrow central line widths as would be expected for helix surface sites (Figure 2, shaded spectra).

The SNARE Motif of Syntaxin in the SNARE Complex. We next investigated whether the structure of the boundary between the interacting layers of the core complex and the linker region is altered when the linker region and the Habc domain are present. In the crystal structure of the core complex (*11*), residue 198 represents the most N-terminal of the interacting layers (layer −8) in which contacts are made between corresponding residues of the N- and C-terminal SNARE motif of SNAP-25 but not synaptobrevin. The few N-terminally adjacent residues of the isolated SNARE motif used for crystallization are also α-helical. To test whether this is also the case when the entire cytoplasmic domain of syntaxin is used for SNARE complex formation, we performed spin labeling of residues 189−195 and 197.

In accordance with the crystal structure of the core complex spin-labeled positions that are pointing toward the interior of the complex (residues 191, 194, and 195) exhibit strong immobilizations as can be seen from the broad spectra (Figure 3). In contrast, helix surface sites (residues 190, 193, and 197) exhibit much higher mobility as evidenced by the sharp and narrowly spaced lines in the EPR spectra. Positions with tertiary contacts (residues 189 and 192) yield multicomponent spectra. As typically seen for these sites, the outer peaks of the spectra compare with those obtained for buried sites, and the inner peaks share similarities with helix surface sites. Furthermore, the spectra obtained for positions 192 and 197 overlap perfectly with those obtained previously when only the SNARE motif instead of the entire cytoplasmic domain was used for SNARE complex formation. Thus, the side chain interactions of the stretch between residues 197 and 189 are not altered when the linker and the Habc domain are present; they are thus accurately represented by the crystal structure of the core complex.

The Linker Region of Syntaxin. To investigate the linker region of syntaxin, single cysteine mutants of almost all positions within this region (residues 146−188) were gener-

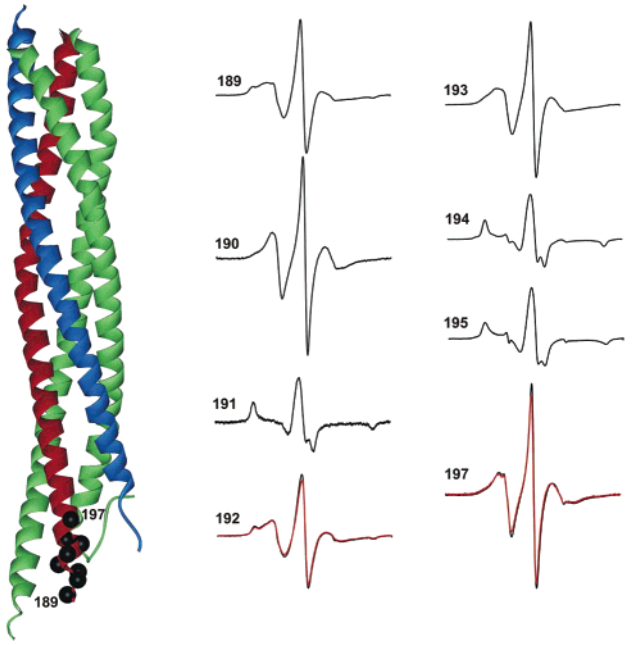

FIGURE 3: EPR spectra of syntaxin (bound to synaptobrevin and SNAP-25) spin labeled at the N-terminal end of the SNARE motif. Labeling positions that were chosen for the EPR analysis are depicted by the corresponding α-carbons in the crystal structure (left).

ated, spin labeled, and assembled into SNARE complexes. The spectra for positions 146−148 (Figure 4) indicate that these amino acids are still partially structured, possibly representing multiple conformations. Note that the NMR data resolve the structure up to amino acid 146, while the helices in the crystal structure are defined up to amino acids 145, 146, and 147, depending on which of the three Habc regions in the elementary cell is analyzed (*16*, *17*). Spectra for positions 149−182 are very narrow, with the outer peaks being separated by less than 36 G, indicating that all of these sites are highly mobile and without secondary structure. Starting at position 183 syntaxin becomes more ordered again. The spectrum of position 185 has two components: a strong immobile component reflected by the outer peaks and a mobile component represented by the inner peaks. It is possible that at this position the N-termini of either SNAP-25 or synaptobrevin collide with syntaxin. Interestingly, a proteinase K digest of the ternary complex revealed cleavage sites in syntaxin prior to amino acids 180 and 184 (*29*). No further cleavage sites were found up to amino acid 262, indicating that the region following amino acid 184 is structured and protected from protease digestion. The next immobilized residue following position 184 is amino acid 188. Positions in between are either surface (residue 186) or tertiary contact (residue 187). Thus, this region of syntaxin shows the characteristics of an α-helix, with a periodicity of three to four amino acids per turn. This periodicity extends into the SNARE motif (see also Figure 3).

Although the extension of the H3 helix in the ternary complex is reminiscent of the extension in the syntaxin/munc18 complex, stabilization underlies different principles. While in the syntaxin/munc18 complex this stretch of H3 is stabilized by interactions with the linker region as well as an extension of the Hc helix, in the SNARE complex stabilization appears to be due to interactions with neighbor-

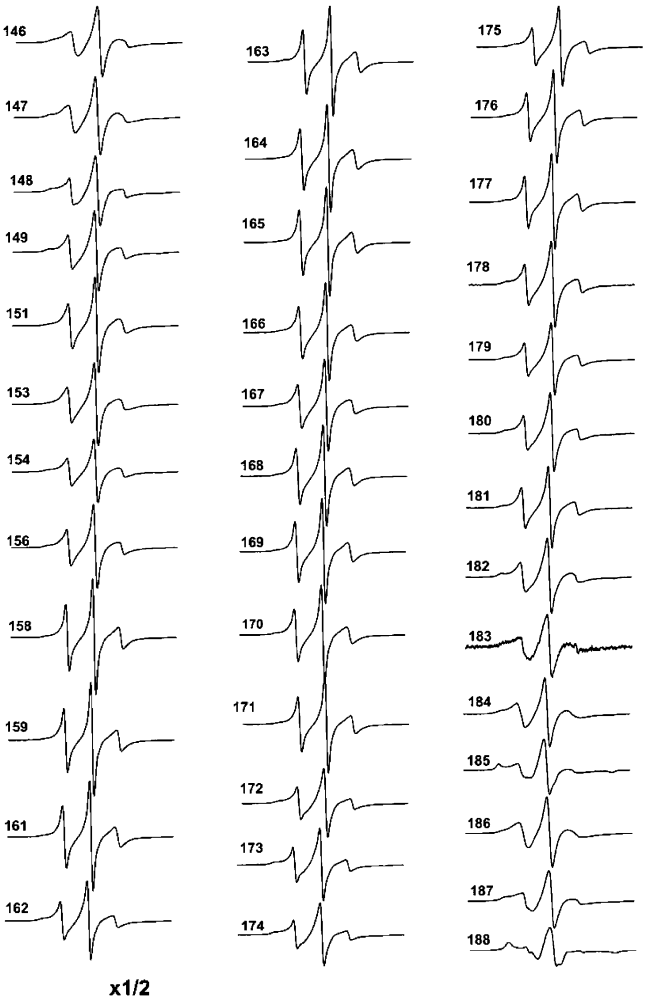

FIGURE 4: EPR spectra of syntaxin (bound to synaptobrevin and SNAP-25) spin labeled in the linker region. Amplitudes are multiplied by $^1/_2$ to facilitate comparison. Note that spectra from position 183 onward are typical for α-helix as observed by the periodicity in the spectra.

ing SNARE proteins. In fact, all additional helices in munc18 appear to participate in an extended network of side chain interactions in which amino acids within the extended Hc domain interact with those in the H3 domain (Figure 5A). In addition, a short linker helix spanning amino acids 162−170 exists, which forms contacts with both the Hc and H3 domains. Also, a contact between munc18 and the linker helix appears to further stabilize the network. H3 residues that are in contact with the helix linker in the syntaxin/munc18 complex form new contacts with partnering SNAREs in the SNARE complex. Thus, absence of contacts with H3 and munc18 suffices to collapse the linker helix and the extension of the Hc helix (Figure 5B). Plotting of the inverse central line widths against residue numbers further emphasizes this point (Figure 6). The entire region of syntaxin in the SNARE complex ranging from amino acid 149 to amino acid 182 is unstructured. We recently showed that most measured positions within the loop between the two SNAP-25 helices had values for the inverse central line width of about 0.4 (*35*). In the case of the syntaxin loop most positions have values around or above 0.4 (residues 149−182), including the region that forms a linker helix in complex with munc-18 (residues 162−170). Thus, this extended region of the syntaxin linker is extremely dynamic. Values

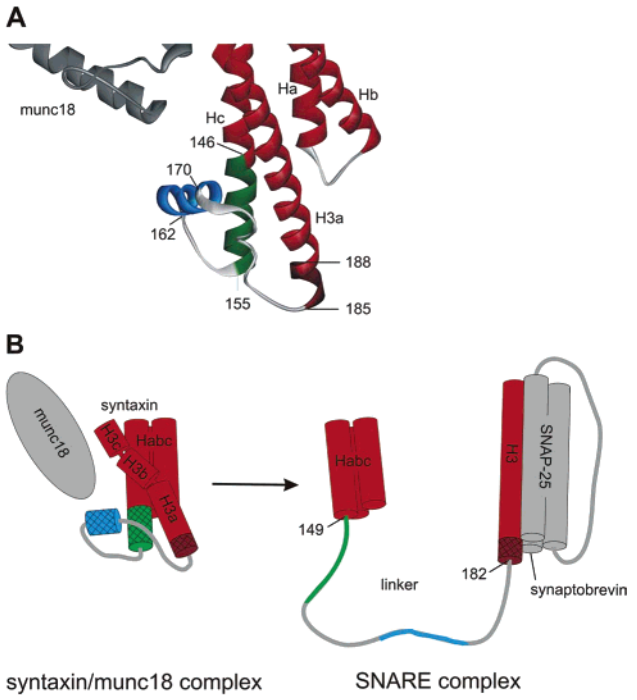

FIGURE 5: Structure of the syntaxin linker. (A) X-ray crystal structure of the syntaxin linker within the syntaxin/munc18 complex (*27*). In the complex with munc18 the linker region of syntaxin (residues 146−188) resembles a network of interactions that involves munc18 (gray), an extended Hc helix (green, residues 146−155), a short linker helix (blue, residues 162−170), an elongation of H3 (dark red, residues 185−188), and the regular H3 and Habc domains (red, residues 189−259 and 27−145, respectively). For a more detailed description of these and additional site chain interactions, see ref *27*. (B) Cartoon depicting the structural changes occurring during the transition from a syntaxin/munc18 complex to a ternary SNARE complex [color coding as in (A)]. Synaptobrevin and SNAP-25 are also depicted in gray. Note that the extended Hc helix and the linker helix collapse, resulting in a completely unstructured region within the linker ranging from amino acids 149−182 and a small partially structured region from amino acids 146−148. The H3 domain is N-terminally extended to amino acid 183.

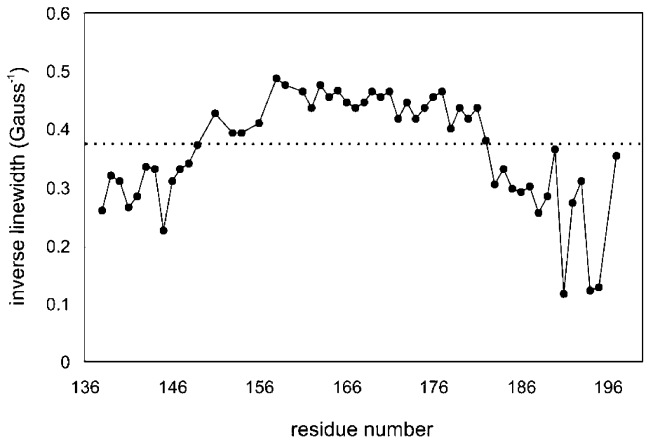

FIGURE 6: Inverse central line width as a measure for backbone structure. The inverse central line widths of the central resonances from all EPR spectra are plotted against the corresponding residue numbers. In general, spin labels attached to residues in the Habc domain and SNARE motif result in lower r^{-1} values than labels attached to the linker region. Within the Habc domain and the SNARE motif the r^{-1} values show a 3−4 periodicity indicative of helical structure. Positions that are buried have lower r^{-1} values than those on the surface. Note that buried residues in the SNARE motif have lower r^{-1} values (helix with very little dynamics) than those in the Habc domain. The dotted line divides unstructured residues from structured ones.

for positions 183−188 are considerably lower and therefore strengthen the view that this part of the linker is structured. Here the inverse line widths are around 0.3 and compare well with those obtained for the Habc domain (residues 138−145) and the immediately neighboring amino acids 146−148. In the case of residues 138−145 helix periodicity becomes apparent and is reflected in low inverse line widths for residues that have helix contacts (residues 138, 141, and 145) and high inverse line widths for those residues that reside on the surface (residues 139, 142, and 143). A similar pattern is observed for positions within the SNARE motif (residues 189−197). Interestingly, immobile positions within the Habc domain (residues 138, 141, and 145) and within the linker region (residues 185 and 188) have higher values than those in the SNARE motif (residues 191, 194, and 195), reflecting more dynamic helices (*42*).

DISCUSSION

Syntaxin 1 is known to cycle between different conformations that are essential for its function in neuronal exocytosis. While the conformational changes associated with assembly and disassembly of the SNARE motifs are well worked out, corresponding information about conformational changes associated with the transition between the open and the closed conformation has been scarce. We have now shown that in the open state the linker region connecting the Habc domain and the SNARE motif in syntaxin 1 is unstructured (with only short partially structured transitions at either end) (Figure 5B). In contrast, both the structure of the Habc domain and the SNARE motifs appear to be identical to those determined by NMR spectroscopy and crystallography of the corresponding fragments.

Our finding that the linker region appears to cycle between random coil (in complex with its SNARE partners) and a defined secondary structure [in complex with munc18 (*27*)] is reminiscent of the conformational cycle of the adjacent SNARE motif (*35*). Several residues within the linker can be either α-helical or random coil, depending on whether syntaxin is in complex with munc18 [α-helical positions: 146−155, 162−170 (*27*)] or with synaptobrevin and SNAP-25 [α-helical positions: 146−149, 183−189 (*11*)]. These structures probably represent snapshots in the reaction coordinate from the closed conformation of syntaxin in complex with munc18 to an open form of syntaxin.

Unfortunately, we were unable to obtain interpretable EPR spectra from uncomplexed syntaxin. This is due to the formation of homooligomeric mixtures that form at higher micromolar concentrations (*17*) (documented by extensive spin−spin coupling), preventing us from studying the structure of the linker region in the free molecule. Using distance determinations by fluorescence resonance energy transfer measurements of single molecules, we have recently shown that free syntaxin rapidly switches between closed and open conformations (Margittai et al., submitted for publication), with the closed and open conformations being similar to those in complex with munc18 and the SNARE partners, respectively. However, detailed information about peptide backbone structures could not be obtained with this fluorescence approach. Thus, it remains to be established

whether assumption of the closed conformation suffices to induce structure in the linker region or else whether contact with munc18 is needed for its stabilization.

A double mutant within the linker region of syntaxin (L165A/E166A) results in reduced binding to munc18 (*25*), underlining the importance of the linker region in the association of both proteins. It is possible that in the cell factors exist that interact with the linker and destabilize the association with munc18.

In yeast, isolated Sso1p (syntaxin homologue) exists in a closed conformation, which shares significant similarities with the closed conformation of syntaxin in complex with munc18 (*20*, *27*). Besides the linker helix it contains an additional short helix that is located C-terminally. Therefore, in yeast stabilization of the linker region does not require the binding of Sec1p (munc18 homologue). Interestingly, Sec1p does not interact with the closed conformation of Sso1p but is thought to bind to the assembled SNARE complex (*43*).

Furthermore, recent evidence has shown that other syntaxins bind to their corresponding munc18 homologues exclusively through their N-terminal regions (*19*, *44*, *45*).

It is thus conceivable that the N-terminal extensions of syntaxins and some of the other SNAREs serve as a scaffold for the recruitment of regulatory proteins that interact, directly or indirectly, with the SNARE complex before or during the fusion reaction. In addition to munc18 and its homologues, several other potential regulators are known to interact with this region, e.g., munc13 (*46*). Thus, flexibility in the linker region may allow for spatial accommodation of structurally different proteins at the fusion site where steric constraints may limit accessibility. Furthermore, it may explain why NSF (which is supposed to bind to the N-terminal end of the four-helix bundle at the beginning of the disassembly reaction) is not hindered by the presence of such N-terminal domains even if there are several of them in a single complex. Further work is required to find out whether the corresponding linker regions of other members of the syntaxin family are also unstructured and, if so, if these regions are capable of conformational switching.

ACKNOWLEDGMENT

We thank Maria Druminski for superb technical assistance.

REFERENCES

1. Chen, Y. A., and Scheller, R. H. (2001) *Nat. Rev. Mol. Cell Biol. 2*, 98−106.
2. Rizo, J., and Sudhof, T. C. (2002) *Nat. Rev. Neurosci. 3*, 641−653.
3. Rettig, J., and Neher, E. (2002) *Science 298*, 781−785.
4. Hanson, P. I., Heuser, J. E., and Jahn, R. (1997) *Curr. Opin. Neurobiol. 7*, 310−315.
5. Jahn, R., and Sudhof, T. C. (1999) *Annu. Rev. Biochem. 68*, 863−911.
6. Lin, R. C., and Scheller, R. H. (2000) *Annu. Rev. Cell Dev. Biol. 16*, 19−49.
7. Hayashi, T., McMahon, H., Yamasaki, S., Binz, T., Hata, Y., Sudhof, T. C., and Niemann, H. (1994) *EMBO J. 13*, 5051−5061.
8. Fasshauer, D., Otto, H., Eliason, W. K., Jahn, R., and Brunger, A. T. (1997) *J. Biol. Chem. 272*, 28036−28041.
9. Rice, L. M., Brennwald, P., and Brunger, A. T. (1997) *FEBS Lett. 415*, 49−55.
10. Antonin, W., Holroyd, C., Fasshauer, D., Pabst, S., Von Mollard, G. F., and Jahn, R. (2000) *EMBO J. 19*, 6453−6464.
11. Sutton, R. B., Fasshauer, D., Jahn, R., and Brunger, A. T. (1998) *Nature 395*, 347−353.
12. Antonin, W., Fasshauer, D., Becker, S., Jahn, R., and Schneider, T. R. (2002) *Nat. Struct. Biol. 9*, 107−111.
13. Fasshauer, D., Sutton, R. B., Brunger, A. T., and Jahn, R. (1998) *Proc. Natl. Acad. Sci. U.S.A. 95*, 15781−15786.
14. Bock, J. B., Matern, H. T., Peden, A. A., and Scheller, R. H. (2001) *Nature 409*, 839−841.
15. Sollner, T., Bennett, M. K., Whiteheart, S. W., Scheller, R. H., and Rothman, J. E. (1993) *Cell 75*, 409−418.
16. Fernandez, I., Ubach, J., Dulubova, I., Zhang, X., Sudhof, T. C., and Rizo, J. (1998) *Cell 94*, 841−849.
17. Lerman, J. C., Robblee, J., Fairman, R., and Hughson, F. M. (2000) *Biochemistry 39*, 8470−8479.
18. Antonin, W., Dulubova, I., Arac, D., Pabst, S., Plitzner, J., Rizo, J., and Jahn, R. (2002) *J. Biol. Chem. 277*, 36449−36456.
19. Dulubova, I., Yamaguchi, T., Wang, Y., Sudhof, T. C., and Rizo, J. (2001) *Nat. Struct. Biol. 8*, 258−264.
20. Munson, M., Chen, X., Cocina, A. E., Schultz, S. M., and Hughson, F. M. (2000) *Nat. Struct. Biol. 7*, 894−902.
21. Misura, K. M., Bock, J. B., Gonzalez, L. C., Jr., Scheller, R. H., and Weis, W. I. (2002) *Proc. Natl. Acad. Sci. U.S.A. 99*, 9184−9189.
22. Verhage, M., Maia, A. S., Plomp, J. J., Brussaard, A. B., Heeroma, J. H., Vermeer, H., Toonen, R. F., Hammer, R. E., van den Berg, T. K., Missler, M., Geuze, H. J., and Sudhof, T. C. (2000) *Science 287*, 864−869.
23. Pevsner, J., Hsu, S. C., Braun, J. E., Calakos, N., Ting, A. E., Bennett, M. K., and Scheller, R. H. (1994) *Neuron 13*, 353−361.
24. Yang, B., Steegmaier, M., Gonzalez, L. C., Jr., and Scheller, R. H. (2000) *J. Cell Biol. 148*, 247−252.
25. Dulubova, I., Sugita, S., Hill, S., Hosaka, M., Fernandez, I., Sudhof, T. C., and Rizo, J. (1999) *EMBO J. 18*, 4372−4382.
26. Richmond, J. E., Weimer, R. M., and Jorgensen, E. M. (2001) *Nature 412*, 338−341.
27. Misura, K. M., Scheller, R. H., and Weis, W. I. (2000) *Nature 404*, 355−362.
28. Inoue, A., Obata, K., and Akagawa, K. (1992) *J. Biol. Chem. 267*, 10613−10619.
29. Fasshauer, D., Eliason, W. K., Brunger, A. T., and Jahn, R. (1998) *Biochemistry 37*, 10354−10362.
30. Poirier, M. A., Hao, J. C., Malkus, P. N., Chan, C., Moore, M. F., King, D. S., and Bennett, M. K. (1998) *J. Biol. Chem. 273*, 11370−11377.
31. Nicholson, K. L., Munson, M., Miller, R. B., Filip, T. J., Fairman, R., and Hughson, F. M. (1998) *Nat. Struct. Biol. 5*, 793−802.
32. Hanson, P. I., Roth, R., Morisaki, H., Jahn, R., and Heuser, J. E. (1997) *Cell 90*, 523−535.
33. Fasshauer, D., Antonin, W., Margittai, M., Pabst, S., and Jahn, R. (1999) *J. Biol. Chem. 274*, 15440−15446.
34. Higuchi, R. (1990) in *PCR Protocols: A Guide to Methods and Applications* (Innis, M. A., Gelfand, D. H., Sinisky, J. J., and White, T. J., Eds.) pp 177−183, Academic Press, New York.
35. Margittai, M., Fasshauer, D., Pabst, S., Jahn, R., and Langen, R. (2001) *J. Biol. Chem. 276*, 13169−13177.
36. Hubbell, W. L., Cafiso, D. S., and Altenbach, C. (2000) *Nat. Struct. Biol. 7*, 735−739.
37. Hubbell, W. L., McHaourab, H. S., Altenbach, C., and Lietzow, M. A. (1996) *Structure 4*, 779−783.
38. Hubbell, W. L., Gross, A., Langen, R., and Lietzow, M. A. (1998) *Curr. Opin. Struct. Biol. 8*, 649−656.
39. Feix, J. B., and Klug, C. S. (1998) *Biol. Magn. Reson. 14*, 251−281.
40. Poirier, M. A., Xiao, W., Macosko, J. C., Chan, C., Shin, Y. K., and Bennett, M. K. (1998) *Nat. Struct. Biol. 5*, 765−769.
41. Xiao, W., Poirier, M. A., Bennett, M. K., and Shin, Y. K. (2001) *Nat. Struct. Biol. 8*, 308−311.
42. Isas, J. M., Langen, R., Haigler, H. T., and Hubbell, W. L. (2002) *Biochemistry 41*, 1464−1473.
43. Carr, C. M., Grote, E., Munson, M., Hughson, F. M., and Novick, P. J. (1999) *J. Cell Biol. 146*, 333−344.
44. Dulubova, I., Yamaguchi, T., Gao, Y., Min, S. W., Huryeva, I., Sudhof, T. C., and Rizo, J. (2002) *EMBO J. 21*, 3620−3631.
45. Bracher, A., and Weissenhorn, W. (2002) *EMBO J. 21*, 6114−6124.
46. Betz, A., Okamoto, M., Benseler, F., and Brose, N. (1997) *J. Biol. Chem. 272*, 2520−2526.

BI027437Z